JOURNAL OF MATERIALS SCIENCE 27 (1992) 511–519

Optical absorption and EPR studies of borate glasses with $PbCrO_4$ and Pb_2CrO_5 microcrystals

S. RAM
LMGP, URA 1109, Ecole Nationale Supérieure de Physique de Grenoble, Domaine Universitaire, BP46, 38402 Saint Martin-d'Heres, France

KANIK RAM
Defence Materials and Stores Research and Development Establishment, DMSRDE P.O., G.T. Road, Kanpur 208 013, India

B. S. SHUKLA
Department of Chemistry, University of Toronto, Toronto, Ontario, Canada M5S 1A1

The optical absorption (in the 400–1000 nm region) and electron paramagnetic resonance (EPR) spectra of $50PbO–20Cr_2O_3–(30-y)B_2O_3–yAl_2O_3$ glasses and those crystallized by suitable thermal treatments have been studied. The results are applied to account for the crystallization process, which revealed the crystalline products due to $PbCrO_4$ and Pb_2CrO_5, and crystallization yield was found to be drastically enhanced (by as much as ~85 vol %) with Al_2O_3 additives. The addition of Al_2O_3 in the present glasses and/or the thermal treatments induce the optical absorption intensity in the visible region at the expense of the near infrared region and reflect a gradual decrease in the EPR linewidth, ΔH, at $g \sim 2$. The chromium in these cases most likely exists in a thermodynamic equilibrium between Cr^{3+} and Cr^{6+} oxidation states and the Al_2O_3 favours the $Cr^{3+} \rightleftharpoons Cr^{6+}$ nucleation transformation to accord with the above observations. In addition, the crystalline $PbCrO_4$ and Pb_2CrO_5 comprise CrO_4^{2-} groups with the Cr^{6+} oxidation state of chromium. This presents a phenomenological correlation for a local symmetry similarity of the CrO_4^{2-} groups in glass and the microcrystalline products and observation of an enhanced crystallization yield due to Pb_2CrO_5 crystallites in the glasses using Al_2O_3 additives. The chromium occupying the tetragonal CrO_4^{2-} anion sites migrates rather easily from the glass (subject to the thermal treatment) to the growing nucleation sites of $PbCrO_4/Pb_2CrO_5$, whereas those Cr^{3+} usually occupying the octahedral sites, which are associated with characteristically large stabilization energy, hardly play a direct role in the crystallization.

1. Introduction

The optical and most other physical properties of the glass-ceramic materials can be substantially modified by the size and morphology of the crystalline grains and their distribution in the glass matrix, and at present much effort is being focused on the development of materials with fine grains [1–3]. During crystallization studies of the chromium-rich materials we found that very fine grains due to the crystalline $PbCrO_4$ or Pb_2CrO_5 can be precipitated out in $50PbO–20Cr_2O_3–(30-y)B_2O_3–yAl_2O_3$ glasses subject to suitable thermal treatments [3]. Small additions of Al_2O_3 (up to 5 mol %) favoured the crystallization of pure Pb_2CrO_5 phase with promisingly sharp distribution of the grains throughout the bulk. Glass-ceramics with such a crystalline structure minimize especially the inhomogeneous variation in the optical signals and improve many other physical properties. Moreover, the glass-ceramics with crystalline products due to the lead chromates have great scope for industrial applications such as polymer emulsion coating, high corrosion resistance, or ultraviolet radiation protective materials, etc. Crystalline Pb_2CrO_5 also exhibits photoconductivity [4–6].

The vibrational analysis using infrared and Raman spectroscopy of these glasses was reported in an earlier investigation [7]. The results decisively demonstrated the effects of Al_2O_3 incorporation on the glass network structure, which modifies the structure indicating $BO_3 \rightleftharpoons BO_4$ group transformation in the structural units. A glass containing $y = 5$ mol % Al_2O_3 revealed an optimum concentration of BO_4 groups in the structural units, which favoured the growth of $Pb_2CrO_5(PbO \cdot PbCrO_4)$ crystals, through the suitable thermal treatments [3], probably, due to local symmetry similarity set-up during the thermal treatments.

We report here the results of the optical absorption and electron paramagnetic resonance (EPR) studies of $50PbO–20Cr_2O_3–(30-y)B_2O_3–yAl_2O_3$ glasses, with

0022–2461/92 $03.00 + .12

$y \leqslant 5$. The data are correlated with the crystallization process which is discussed in terms of the variation of $Cr^{3+} \rightleftharpoons Cr^{6+}$ oxidation state of chromium.

2. Experimental procedure

The glasses, represented by $50PbO–20Cr_2O_3–(30-y)B_2O_3–yAl_2O_3$, with $y < 5$, were prepared by rapidly quenching a molten mixture of reagent-grade chemicals (PbO, Cr_2O_3, H_3BO_3 and Al_2O_3) at room temperature. They were pressed between two stainless steel plates to thin platelets of ~ 0.05 cm thickness. The crystallization of the various glasses with $PbCrO_4$ or Pb_2CrO_5 as the prominent microcrystalline phase, was performed by giving thermal treatment at the elevated temperatures determined from the thermal analysis [3].

Optical absorption spectra of the various as-quenched and crystallized glasses were studied (in the region 400–1000 nm) using a Cary 2300 spectrophotometer and an optical multichannel analyser. The light beam was focused on the sample to a small size compared with that of the excitation beam so that only a uniformly excited zone is probed. The specimens were polished using a diamond polishing powder and finally with 0.3 μm Al_2O_3 powder to ensure an optically flat surface and with a thickness that allowed absorption of the sample within the measurable range of the spectrophotometer.

The EPR spectra were recorded on a Varian Associates spectrophotometer (model 109) in X-band frequency ($f = 9.4$ GHz) region. The applied magnetic field, which was varied from 0–10 kOe, was calibrated with a digital nuclear magnetic resonance gaussmeter (Varian E-500) and was modulated with 100 kHz for EPR detection. The frequency of the resonance cavity was measured by a DPPH marker at $g = 2.000\,36$.

3. Results and discussion

3.1. Optical absorption studies

The $50PbO–20Cr_2O_3–30B_2O_3$ glasses absorb strongly in the near ultraviolet to visible regions (400–800 nm) which is followed by characteristically weaker absorption in the near infrared region (above 800 nm). The absorption spectra (400–1000 nm) obtained for (a) an as-quenched glass, and glasses heat-treated at (b) 500 °C, and (c) 700 °C for 2 h are shown in Fig. 1. The heat-treatment of the glass induces the absorption in the visible and near ultraviolet regions (starts from 800 nm and grows continuously towards the ultraviolet region) at the expense of the absorption intensity in the near infrared region. This makes the product practically useful for optical glasses/filters or as a coating material of different absorption grades for the visible radiation and with almost transparent behaviour for the near infrared radiation. Glasses (b) and (c) reflect a sufficiently wide region of practically constant absorption between 540 and 740 nm which was little affected by heating at temperatures as high as 700 °C. These glasses, however, become soft and begin to stick to the container above 700 °C. A quite flat absorption region between 400 and 700 nm is also shown for the as-quenched glass (a), which is very sensitive to the atmosphere. The surface of the glass is readily oxidized and the absorption differs moderately.

Fig. 2 shows the absorption spectra of glasses containing Al_2O_3 additives which appear to affect very critically both the positions and intensities of the absorption maxima. The absorbance is decreased by approximately three times in the region below 820 nm and is enhanced by approximately five times in the 650 nm region, on adding 1 or 5 mol % Al_2O_3. Moreover, the spectrum evolves growth of at least two different absorption bands overlapping in the 550–800 nm region. More or less similar results were also observed on heat-treatment of the $50PbO–20Cr_2O_3–30B_2O_3$ glass containing no Al_2O_3 additive. This indicates a close similarity in the variation of oxidation state and/or local symmetry of the chromium ions (responsible for the absorption in this spectrum) in the glass through these two processes.

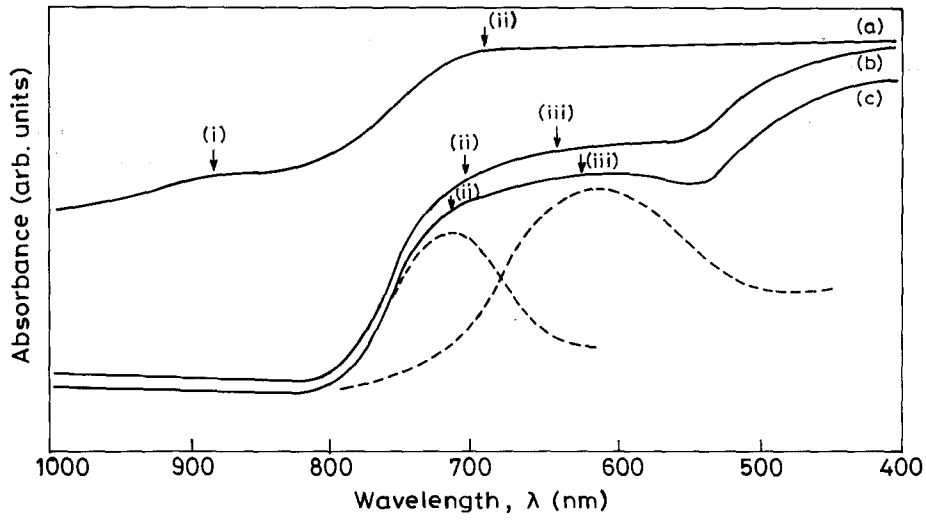

Figure 1 Optical absorption spectra of $50PbO–20Cr_2O_3–30B_2O_3$ glasses: (a) as-quenched, (b, c) after heating at 500 °C/2 h and 700 °C/2 h, respectively. The arrows indicate average positions of the absorption maxima analysed using a Lorentzian shape for them. The complete analysed shapes of the absorption maxima (ii) and (iii) are also shown by the dotted lines in the case of spectrum c.

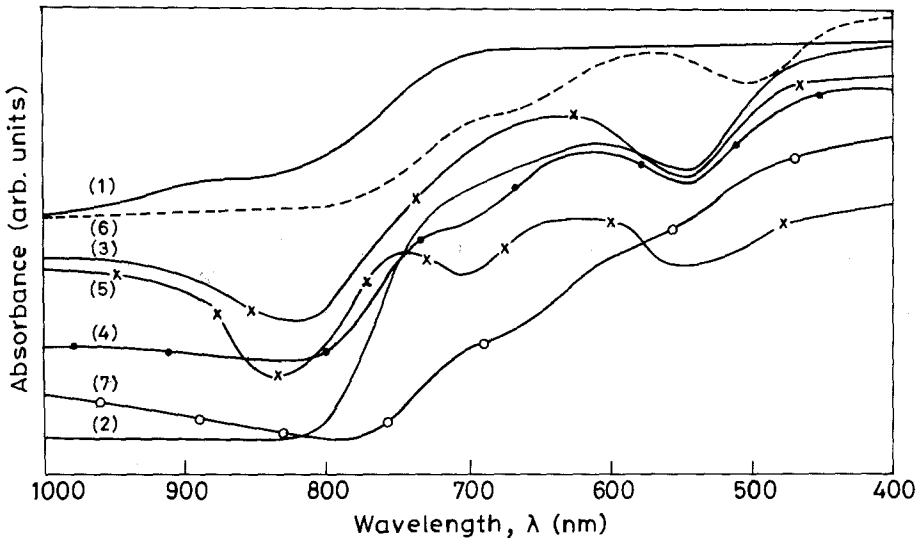

Figure 2 Effect of Al_2O_3 addition on the optical absorption spectra of $50PbO–20Cr_2O_3–(30-y)B_2O_3–yAl_2O_3$ glasses. Spectra 1–4 are recorded from the glasses containing $y = 0$, 1, 3 and 5 mol % Al_2O_3, respectively. Spectrum 5 is recorded after heating the glass of composition $y = 3$ at 900 °C/25 h. Spectra 6 and 7 are recorded after heating the glass of composition $y = 5$ at 850 and 1200 °C for 25 h, respectively.

The network structure in these glasses is composed of essentially diborate/triborate units with BO_3 and BO_4 groups [7–9]. Vibrational analysis [7], particularly using the Raman spectroscopy, has been very rewarding for assigning the structural units. The Raman spectrum revealed characteristically sharp stretching bands due to BO_3 and BO_4 groups at 810 and 780 cm^{-1}, respectively; their relative intensities vary drastically subject to Al_2O_3 incorporation in the various glasses and account well for $BO_3 \rightleftharpoons BO_4$ group transformation in the structural units. The ratio estimated for BO_4 and BO_3 groups was found to be maximum (~ 2.3) for the glass with $y = 5$ mol % Al_2O_3. Thermal treatment of these glasses at temperatures between 500 and 1200 °C produces crystalline $PbCrO_4$ or Pb_2CrO_5 as the prominent crystalline phase, determined from the X-ray diffractometry (see Fig. 3). Both of the crystalline products comprise CrO_4^{2-} groups with the oxidation state of chromium as Cr^{6+}. Thus the local structures for CrO_4 and BO_4

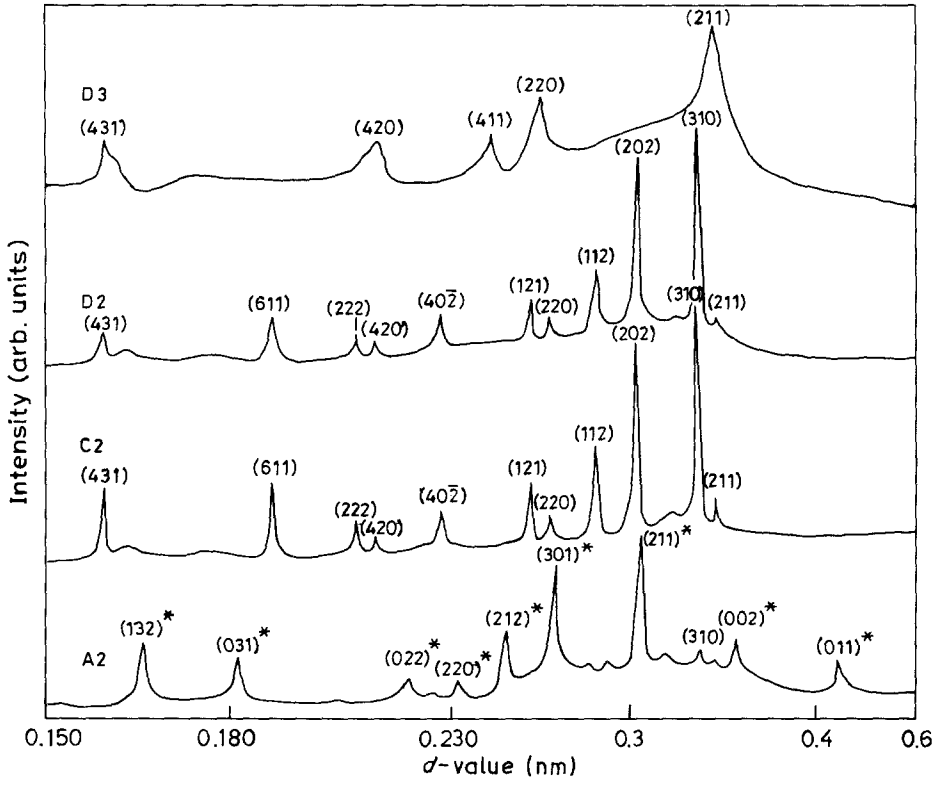

Figure 3 X-ray powder diffraction patterns of the various heat-treated glasses. A2, 700 °C/2 h; C2, 900 °C/25 h; D3, 1200 °C/25 h. The prominent diffraction lines are marked by the ($h\,k\,l$) values of the crystallized $PbCrO_4$ (*) and Pb_2CrO_5 phases. Note that the characteristically sharp diffraction lines due to Pb_2CrO_5 are obtained for glasses C2 and D2 which contain 3 and 5 mol % Al_2O_3 respectively. The diffraction lines become broad and diffuse on heating at considerably higher temperature in Sample D3, which infers growth of distortion/strain defects in the crystal lattice.

TABLE I Heat-treatment schedules, crystallization, and optical absorption spectra of $50PbO–20Cr_2O_3–(30-y)B_2O_3–yAl_2O_3$ glasses

Composition	Heat-treatment	Sample	Crystalline products	Amount crystallized (vol %)[a]	Absorption maxima[b] (nm)		
					(i)	(ii)	(iii)
$y \sim 0$	As-prepared glass	A0	None	0	890 (9)	694 (46)	—
	500 °C/2 h	A1	$PbCrO_4$ Pb_2CrO_5	15	—	705 (67)	640 (74)
	700 °C/2 h	A2	Same as A1	40	—	715 (59)	626 (69)
$y \sim 1$	As-prepared glass	B0	None	0	—	717 (78)	616 (100)
	500 °C/2 h	B1	Pb_2CrO_5	20	—	720 (75)	620 (95)
	850 °C/25 h	B2	Pb_2CrO_5	45	—	725 (70)	620 (90)
$y \sim 3$	As-prepared glass	C0	None	0	—	723 (43)	633 (61)
	900 °C/25 h	C2	Pb_2CrO_5	80	—	748 (40)	626 (46)
	1200 °C/25 h	C3	$nPbO \cdot PbCrO_4$	85	—	750 (40)	630 (50)
$y \sim 5$	As-prepared glass	D0	None	0	—	730 (37)	625 (60)
	500 °C/2 h	D1	Pb_2CrO_5	25	—	730 (35)	625 (50)
	850 °C/25 h	D2	Pb_2CrO_5	80	—	694 (26)	578 (41)
	1200 °C/25 h	D3	$nPbO \cdot PbCrO_4$	85	—	694 (30)	588 (60)

[a] Crystallized volume fraction was estimated using optical/electron microscopy as discussed in [3].

[b] The peak intensities of the absorption maxima are given in parentheses, assuming a 100 unit intensity for the most intense absorption at 616 nm in sample B0. A thickness of about 60 μm was used for all the samples in the present measurements.

groups in the glass can be treated as symmetrically similar, as far as the amorphous (random) structure of the material is concerned. Glass is material in an unstable state and relaxation towards an equilibrium state of low energy (but still amorphous) occurs by local structural changes in the structural units. Crystallization of glass is a further advanced stage of the stabilization of energy. Quite often the growth of BO_4 groups induced by incorporation of Al_2O_3 in the glasses causes nucleation of CrO_4 groups in order to minimize the structural energy and disorder. In fact, the concentrations of CrO_4 groups may be as much as those induced by the crystallization of $50PbO–20Cr_2O_3–30B_2O_3$ glass. The similarity observed for their optical spectra is phenomenological in this model.

The positions of the absorption maxima and their peak intensities observed for the various as-prepared and heat-treated glasses are summarized in Table I. The schedule of heat-treatments and the results of crystallization are also included in the table. The weak absorption peak at 890 nm (indicated by an arrow in Fig. 1) and the characteristically strong absorption group observed at ~ 700 nm for the $50PbO–20Cr_2O_3–30B_2O_3$ glass are intrinsic to $d \rightarrow d$ electronic transitions (corresponding to $^4A_2 \rightarrow {}^4T_2$ and $^4A_2 \rightarrow {}^2E, {}^2T_1$ transitions) of Cr^{3+} ($3d^3$). In phosphate or silicate glasses also, the chromium cations have been shown to exhibit usually two absorption bands in this region [10–14]. The weak intensity observed for the first absorption maximum, which is spin-allowed, indicates small concentration of chromium present as Cr^{3+} in the glass.

The 700 nm band-group, assigned for the spin-forbidden $^4A_2 \rightarrow {}^2E, {}^2T_1$ transitions of Cr^{3+}, comprises an ambiguously strong intensity which also occurs prominently in the glasses containing Al_2O_3 additives and crystallized by thermal treatments. In principle, all these transitions are forbidden [15], but they appear due to mixing of the free ion wavefunctions with those for the neighbour ions or the lattice vibrations. It is likely that the chromium in the present glasses exists in a thermodynamic $Cr^{3+} \rightleftharpoons Cr^{6+}$ equilibrium, with Cr^{3+} and Cr^{6+} oxidation states, and the incorporation of Al_2O_3 additives and/or the thermal treatments induce growth of the $Cr^{6+}(CrO_4^{2-})$, as proposed earlier. The presence of chromium in the different oxidation states allows their intermixing through spin coupling which would reveal modified energy levels of the coupled ion-pairs. The energy levels for the ground and excited states of isolated Cr^{3+} and Cr^{6+} ions are portrayed in Fig. 4. The transition between ground state $^4A_2$ and the excited state ^2E or $^2T_1$ of Cr^{3+} or that between ground state $^1A_1$ and the first excited state $^3A_2$ of Cr^{6+} is forbidden by both symmetry as well as spin. As the electrons of Cr^{3+} couple with those of Cr^{6+}, the transition between the excited and ground states becomes spin-allowed, as shown in Fig. 4, for the "Cr^{3+}–Cr^{6+}" coupled pair, accounting for the large intensity of the 700 nm band group observed in the present samples. Formation of similar coupled "ion-pairs" in Mn^{2+}-doped $RbMgF_3$ crystals [16] led to

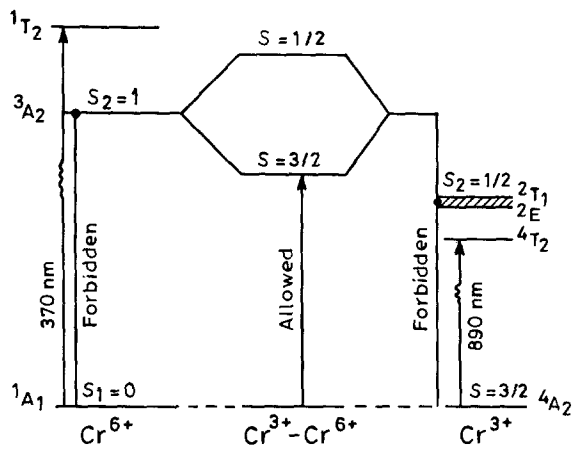

Figure 4 Schematic diagram for spin coupling between the ground and $^3A_2$ and ^2E, $^2T_1$ excited states of isolated Cr^{6+} and Cr^{3+}. The shaded area indicates the overlapping region between ^2E and $^2T_1$ excited states of Cr^{3+}. The energy levels for Cr^{3+} and Cr^{6+} oxidation states of chromium are taken from [15] and [18], respectively.

the intensity of a spin-forbidden $^6A_{1g} \rightarrow {}^4T_{1g}$ transition of Mn^{2+} being enhanced by a factor of 10^5.

A required condition for mixing of the free-ion wavefunctions with those of the neighbour ions or the lattice vibrations is that the symmetry associated with the centre of inversion be destroyed by the neighbours. This is evident from our vibrational analysis of the various glasses, where the degeneracies of ν_2(E) and ν_3, ν_4 (F_2) vibrational modes of CrO_4^{2-} were found to be removed completely, confirming a site symmetry for CrO_4^{2-} lower than a T_d symmetry [7]. This may be accomplished both dynamically (via odd-parity vibrations) and statistically (as a result of the odd-parity distortions present in the system). The broadness as well as the intensity of the absorption maximum at 700 nm increases due to incorporation of Al_2O_3 in the glasses, which is an example of the dynamically induced intensity mechanism [17]. The Al_2O_3 additives (which behave as a glass network modifier) cause non-bridging oxygens and produce heterogeneous nucleation centres in the glass, separating and reducing the long-range orders of the chromium (and also borate) groups. This must allow better chances of mixing of the electronic transitions with the lattice vibrations because the valence Cr-electrons in that case are confined mainly to the chromium CrO_4^{2-} centres. Moreover, as the chromium with non-bridging oxygens binds an excited electron less tightly than that with the bridging oxygens, the absorption maximum shifts considerably to smaller energies (longer wavelengths) with the addition of Al_2O_3 in these glasses (see Fig. 2 and Table I).

These transitions were also studied by recording the spectra at different temperatures between 77 and 450 K. Their intensities (integrated) were observed to increase regularly with increasing temperature, showing an $\sim 50\%$ increase on raising the temperature from 295 to 450 K. This supports the fact that the associated transitions have an intensity basically owing to the dynamically induced intensity mechanism; because at higher temperatures, more of the

odd-parity vibrations become populated and the average odd-parity distortion is increased.

The crystalline products due to $PbCrO_4$ or Pb_2CrO_5 observed in these glasses can also exhibit charge transfer bands characteristic of the CrO_4^{2-} chromophore, but they lie far below in the ultraviolet region [18]. Moreover, Toda and Morita [4–6] reported that Pb_2CrO_5 shows photoconduction with an optical bandgap energy $E_p \simeq 2.1$ eV (or at 570 nm). Indeed a strong absorption group occurs, around 600 nm for our Al_2O_3-containing glasses, due to an electronic excitation through this optical bandgap. The position of the absorption maximum is very sensitive to the impurities being incorporated into the Pb_2CrO_5 microcrystals during the crystallization. Glass-ceramic sample D_2, which contains $\sim 80\%$ crystallized volume fraction due to Pb_2CrO_5 as the only crystalline phase, shows an absorption maximum at 578 nm, which is fairly consistent with the optical bandgap determined by the photoconduction measurements on the pure Pb_2CrO_5 crystals.

The spectrum loses the band structures embedded in strong continuous absorption, which grows rapidly on the lower wavelengths side, on heating the samples at relatively higher (> 1000 °C) temperatures. This is an example of the intensity enhancement prominently by odd-parity distortion. These specimens incorporate excess PbO in the crystallites following the nPbO + $PbCrO_4 \rightleftharpoons n$PbO · $PbCrO_4$ type substitution reaction, with $n \geqslant 2$. They usually have a twinned or otherwise distorted crystal structure, reflected by the characteristically broad and diffuse diffraction lines, as shown for a representative sample, D_3, in Fig. 3. In that case, the heavy lead sites are also expected to have a distorted metallic lead lattice [19]. It is interesting to note that the optical absorption spectroscopy accounts well for the effects of twinned/distorted crystal lattice, showing as expected broad and diffuse band features, in the spectrum 7 of Fig. 2, for specimen D_3 heated at 1200 °C for 25 h. The continuous absorption probably represents a tail of the CrO_4^{2-} charge transfer bands in the ultraviolet region superimposed on weak electronic transitions between localized states (being allowed due to the odd-parity distortions) in the bandedge tails. Relatively pure and perfect microcrystals of Pb_2CrO_5 were obtained by heating the glass containing 5 mol % Al_2O_3 at appropriately lower temperatures, for example, at 850 °C for 25 h, and the product exhibited characteristically sharp diffraction lines (Fig. 3) and two well-resolved absorption maxima at $\sim$ 578 and 700 nm superimposed on a characteristically much weaker continuous background absorption.

3.2. EPR studies

EPR spectroscopy is a very useful tool for the study of amorphous or crystalline materials with magnetic centres which may be due to anion, cation or a hole centre trapped in material [20–22]. The $50PbO–20Cr_2O_3–(30\text{-}y)B_2O_3–yAl_2O_3$ glasses and those crystallized using the thermal treatments have plausible magnetic centres due to the Cr^{3+} and Cr^{6+} oxidation states of chromium. They exhibit a sharp and single resonance peak of a completely symmetric shape at $g \sim 2$, as shown in Fig. 5. Signal recordings were studied at a sufficiently expanded scale; they did not reveal any splitting or asymmetry in the shape of the signal,

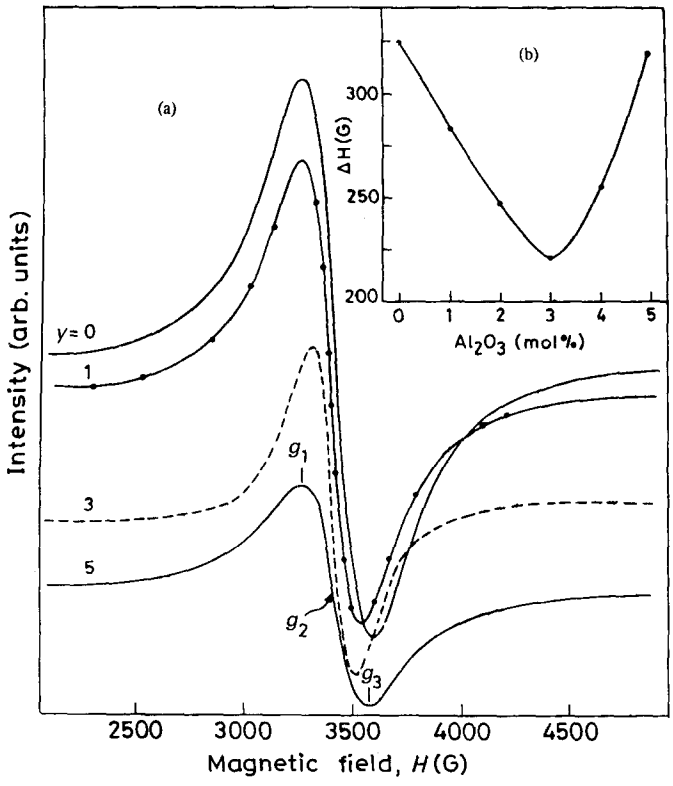

Figure 5 (a) EPR spectra of the various as-quenched $50PbO–20Cr_2O_3–(30\text{-}y)B_2O_3–yAl_2O_3$ glasses. (b) Variation of the linewidth, ΔH, obtained as a function of Al_2O_3 content, y. ΔH shows a minimum for $y = 3$ mol % Al_2O_3 addition in the composition series.

confirming a strong mixing between the Cr^{3+} and Cr^{6+} cations, elucidated by absorption spectroscopy. Also, in a high T_c $YBa_2Cu_3O_7$ superconductor, the different oxidation states of copper (Cu^{3+} and Cu^{2+}) similarly mix together resulting in a single resonance peak at $g \sim 2$. Moreover, Ardelean *et al.* [23] studied EPR of PbO–Cr_2O_3–B_2O_3 glasses when the content of $Cr_2O_3(x)$ varied from 0–35 mol %. They observed that the intensity of the resonance peak decreases gradually with decreasing x, showing a doublet splitting structure, for $x < 10$, followed by a characteristically sharp and single peak at $g \sim 1.97$, for $x \leqslant 1$. According to these authors, the latter resonance peak corresponds to the presence of Cr^{5+} in the glasses. The results, of course, support our conjecture that the chromium in PbO–Cr_2O_3–B_2O_3 glasses exists in a thermodynamic equilibrium with its different oxidation states and those sensitively vary with composition and/or thermal treatment of the glass.

The average position of the resonance does not vary much on incorporation of Al_2O_3 in these glasses. So in order to analyse the structural changes caused by Al_2O_3 incorporation, we measured the g-values at three different positions, g_1, g_2 and g_3 (as shown in Fig. 5), the linewidth ΔH, and the intensity I, for the area within the absorption peak. The results are given in Table II. The intensity, I, was estimated by using a correlation [23]

$$I = (\Delta H)^2 \Delta h \qquad (1)$$

with the ΔH, where Δh refers to peak-to-peak height in the resonance, and was found to be fairly consistent with the graphical area in the resonance peak, within an error of $\pm$ 5%.

The values of I (Table II) were found to decrease on incorporation of Al_2O_3 ($y \leqslant 3$mol %), probably leading to the homogenization and uniform distribution of cations in the glass. A more striking observation of this measurement is represented by the variation of ΔH with y, shown in the inset of Fig. 5: ΔH passes through a minimum for $y \sim 3$. A decrease in ΔH is possible for growth of a crystalline anisotropy if the glass is devitrified during quenching, but the samples examined by X-ray diffractometry and electron microscopy did not indicate the presence of crystalline particles. Thus the only alternative remaining is that the variation of ΔH arises due to $Cr^{3+} \rightleftharpoons Cr^{6+}$ transformation. As the incorporation of Al_2O_3 in the glass favours nucleation of Cr^{6+}, the ratio of Cr^{6+} to Cr^{3+} cations probably approaches a maximum for $y \sim 3$, reflecting a minimum ΔH value; ΔH arises solely due to magnetic-dipole interactions of different chromium sites coupled by exchange interactions [24]. The Cr^{6+} (A) sites bear characteristically smaller magnetic moment than the Cr^{3+} (B) (which comprises a magnetization of $3\mu_B$ intrinsic to $3d^3$ electrons). Accordingly, the AB magnetic interaction decreases on Al_2O_3 addition, and ΔH decreases.

Further, addition of Al_2O_3 by more than an optimum value of $y \sim 3$ mol % in the glass causes distortion of CrO_4^{2-} interstitial sites which accords with the increase of ΔH. The distorted CrO_4^{2-} sites do not appear to participate in the crystallization of the glass appreciably and in fact those compositions did not reveal much crystallization yields. The glasses containing effectively small Al_2O_3 additives of < 5 mol % revealed a quite good crystallization yield (see Table I) with Pb_2CrO_5 ($PbO \cdot CrO_4$) microcrystals, subject to the proper thermal treatments. It appears to be phenomenological that the Al_2O_3 additive causes nucleation of tetragonal CrO_4^{2-} anions which grow prominently into Pb_2CrO_5 crystals during the thermal treatments. The glasses without Al_2O_3 additives comprise mostly the Cr^{3+} cations, which exist essentially in the energetically stabilized octahedral sites [25] and thus hardly take part in the crystallization. This is consistent with the symmetry of the crystallites of Pb_2CrO_5 which have a monoclinic crystal structure (space group C_{2h}^2–C^2/m) comprising tetragonal CrO_4^{2-} anion sites with $Z = 4$ formula units contained in the unit cell [26].

TABLE II g values, linewidth, ΔH, and relative intensity, I, for the resonance observed in various as-prepared and heat-treated $50PbO$–$20Cr_2O_3$–$(30\text{-}y)B_2O_3$–yAl_2O_3 glasses

Composition	Sample	g values			ΔH (G)	I^a
		g_1	g_2	g_3		
$y = 0$	A0	2.073	1.975	1.885	325	100
	A1	2.084	1.958	1.847	416	120
	A2	2.084	1.958	1.846	418	130
$y = 1$	B0	2.072	1.986	1.906	283	64
	B1	2.071	1.980	1.897	300	67
	B2	2.071	1.979	1.895	303	75
	B3	2.071	1.980	1.897	300	80
$y = 3$	C0	2.043	1.977	1.916	220	27
	C2	2.040	1.959	1.885	273	70
	C3	2.040	1.973	1.910	225	80
$y = 5$	D0	2.062	1.966	1.878	320	39
	D1	2.059	1.964	1.877	318	40
	D2	2.040	1.924	1.820	400	70
	D3	2.040	1.977	1.917	212	90
	D4	2.045	1.991	1.940	178	120

[a] Intensity I is expressed in relative unit by assuming a 100 unit intensity for the resonance observed in an as-prepared glass A0. I is normalized in each case for a unit mass of the sample.

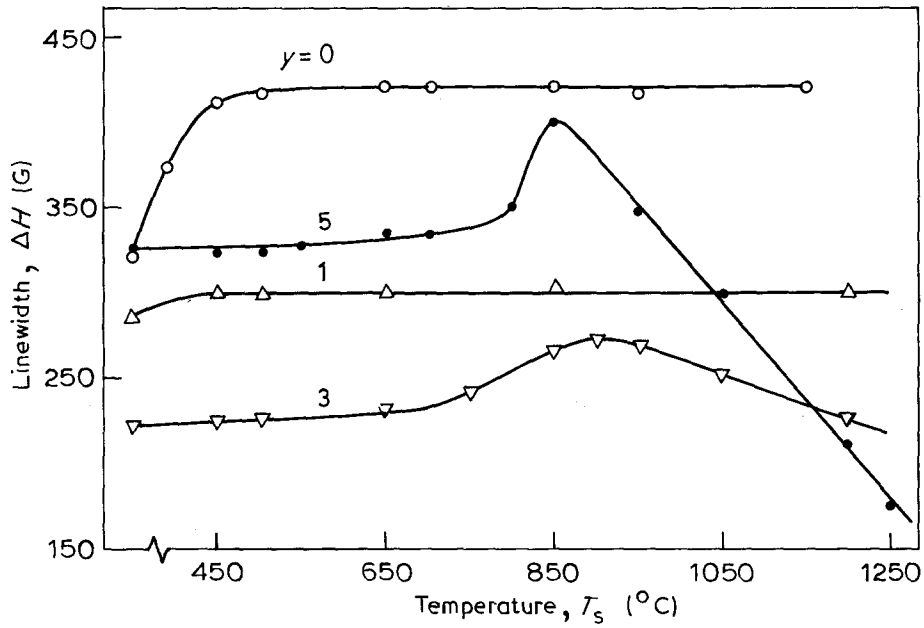

Figure 6 Variation of EPR linewidth, ΔH, in $50PbO{-}20Cr_2O_3{-}(30\text{-}y)B_2O_3{-}yAl_2O_3$ glasses as a function of thermal treatment temperature, T_s, used in the crystallization experiments.

We may now comment on the variation of g-values associated with the structural change around chromium sites. It is well known that for a cubic crystal field with a tetragonal distortion and effective spin $S = 1/2$,

$$g_{\parallel} = 2\text{-}8\frac{\lambda}{\Delta}, \quad g_{\perp} = 2\text{-}2\frac{\lambda}{\Delta} \tag{2}$$

or

$$g_{\parallel} = 2\text{-}6\frac{\lambda}{\Delta}, \quad g_{\perp} = 2 \tag{3}$$

where λ is the spin-orbit coupling constant and Δ the cubic crystal field splitting [20]. Our data for g-values given in Table II follow the order $g_{\perp}$ $(g_1) > g_{\parallel}$ (g_3), with $g_1 \sim 2.0$, excluding the first possibility. This means that the unpaired electron in Cr^{3+} occupies the $X^2{-}Y^2 >$ orbital ground state. The value for $g_{\perp}$ approaches the free ion value ($g = 2$) for the addition of $\leqslant 3$ mol % Al_2O_3 and performing the crystallization of the various glasses, demonstrating $Cr^{3+} \rightleftharpoons Cr^{6+}(CrO_4^{2-})$ cation transformation, which leads the local structure around the chromium sites to change from an octahedral to the tetragonal CrO_4^{2-} symmetry.

Fig. 6 shows the variation of ΔH obtained by crystallization of the glasses at different temperatures, T_s. ΔH increases slowly on raising T_s to 500 °C for Glass A_0, and that containing 1 mol % Al_2O_3 (Glass A1). It predicts emigration of CrO_4^{2-} sites from glassy structure to the crystalline products of $PbCrO_4$ and/or Pb_2CrO_5 in the crystallization process. The crystallization causes non-bridging oxygens in the glass, which eventually offer a redistribution of the glass structure. The Cr-sites, with those non-bridging oxygens, exhibit characteristically stronger magnetic interactions leading to the increase in ΔH. A considerably larger crystallization appeared on heating the glass at higher T_s, but this does not impart significant variation in ΔH, as the non-bridging oxygens have sufficient thermal energy to establish redistribution of the structure.

The effect of crystallization is reflected in the appearance of a peak in the variation of ΔH with T_s at ~ 965 and 900 °C for glasses A3 and A5, containing 3 and 5 mol % Al_2O_3, respectively. They exhibited maximum crystallization of ~ 35 vol % by heating at these temperatures for 25 h. As the heating at lower temperatures induces small crystallization and that at the higher temperatures incorporates boron impurities in the crystallites, the sample comprises small ΔH in either case. A large value of ΔH observed for Samples A3 and A5 is intrinsic to a large magnetocrystalline anisotropy, H_a (which usually decreases by the incorporation of nonmagnetic impurities in the interstitial sites), for the crystalline products [27].

4. Conclusion

In the $PbO{-}Cr_2O_3{-}B_2O_3$ glasses the chromium exists in different oxidation states, prominently due to Cr^{3+} and Cr^{6+}, as analysed by optical absorption and EPR studies. Incorporation of Al_2O_3 additives (effectively < 5 mol %) in these glasses favours nucleation of the latter oxidation state with tetragonal CrO_4^{2-} anion sites which grow into Pb_2CrO_5 (also denoted $PbO \cdot PbCrO_4$) microcrystals, subject to the crystallization by thermal treatment, leading to a markedly enhanced crystallization volume per cent observed for those glasses. Further, the chromium in Pb_2CrO_5 crystals appears as CrO_4^{2-} sites. It shows a phenomenological correlation between the local symmetry similarities for CrO_4^{2-} sites in glass and the microcrystalline Pb_2CrO_5 structure, and the observation of an enhanced crystallization volume per cent due to the latter in the Al_2O_3-containing glasses. The chromium

occupying CrO_4^{2-} sites in the glass requires a characteristically small activation energy (E_J) to cross over the barrier of amorphous $\rightleftharpoons$ crystalline state transformation, and in fact they readily migrate from the glass to the growing Pb_2CrO_5 crystalline sites, subject to suitable thermal treatments. Moreover, the incipient content of chromium present as Cr^{3+} occupies essentially the octahedral sites, which are associated with characteristically large stabilization energy [25], and hardly take part in the crystallization of Pb_2CrO_5.

References

1. L. E. BRUS, *IEEE J. Quant. Electron.* **22** (1986) 1909.
2. P. ROUSSIGNOL, D. RICORD, C. FLYTZANIS and N. NEUROTH, *Phys. Rev. Lett.* **62** (1989) 312.
3. S. RAM and K. A. NARAYAN, *Ind. Engng Chem. Res.* **26** (1987) 1051.
4. K. TODA and S. MORITA, *Appl. Phys. A* **33** (1984) 231.
5. S. MORITA and K. TODA, *J. Appl. Phys.* **55** (1984) 2733.
6. K. TODA and S. MORITA, *ibid.* **57** (1985) 5325.
7. S. RAM and K. RAM, *J. Mater. Sci.* **23** (1988) 4541.
8. M. IRION, M. CAUZI, A. LEVASSEUR, J. M. REAU and J. C. BRETHOUS, *J. Solid State Chem.* **31** (1980) 285.
9. Y. ITO, K. MIYAUCHI and T. OI, *J. Non-Cryst. Solids* **57** (1983) 389.
10. R. J. LANDRY, J. T. FOURNIER and C. G. YOUNG, *J. Chem. Phys.* **46** (1967) 1285.
11. S. A. BRAWER and W. B. WHITE, *J. Chem. Phys.* **67** (1977) 2043.
12. A. LEMPICKI, L. ANDREWS, S. J. NETTEL, B. C. McCOLLUM and E. J. SOLOMON, *Phys. Rev. Lett.* **44** (1980) 1234.
13. L. J. ANDREWS, A. LEMPICKI and B. C. McCOLLUM, *J. Chem. Phys.* **74** (1981) 5526.
14. F. DURVILLE, B. CHAMPAGNON, E. DUVAL and G. BOULON, *J. Phys. Chem. Solids* **46** (1985) 701.
15. S. SUGANO, Y. TANABE and H. HAMIMURA, "Multiples of Transition Metal Ions in Crystals" (Academic Press, New York, 1970).
16. D. K. SARDAR, M. D. SHINN and W. A. SIBLEY, *Phys. Rev. B* **26** (1982) 2382.
17. A. M. STONEHAM, "Theory of Defects in Solids" (Oxford University Press, Oxford, 1975).
18. M. WOLFSBERG and L. HELMHOLZ, *J. Chem. Phys.* **20** (1952) 837.
19. B. F. MENTZEN, A. LATRACH, J. BOUIX and A. W. HEWART, *Mater. Res. Bull.* **19** (1984) 549.
20. A. ABRAGAM and B. BLEANEY, "Electron Paramagnetic Resonance of Transition Ions" (Clarendon Press, Oxford, 1970).
21. D. L. GRISCOM, *J. Non-Cryst. Solids* **13** (1973–74) 251.
22. J. S. THORP and W. HUTTON, *J. Phys. Chem. Solids* **42** (1981) 843.
23. I. ARDELEAN, G. ILONGA, M. PETEANU, E. BARBOS and E. INDREA, *J. Mater. Sci.* **17** (1982) 1988.
24. J. C. M. HENNING and H. Van Den BOOM, *Phys. Rev. B* **8** (1973) 2255.
25. A. J. WOJTOWICZ and A. LEMPICKI, *ibid.* **39** (1989) 8695.
26. J. C. RUCKMAN, R. T. W. MORRISON and R. H. BUCK, *J. Chem. Soc. Dalton Trans.* **1** (1972) 426.
27. S. RAM, *J. Magn. Mater.* **82** (1989) 129.

Received 27 September 1990
and accepted 18 March 1991